XLIII CILAMCE
21–25, November, 2022
FOZ DO IGUAÇU – PR – BRAZIL

Nonlinear Kirchhoff-Love Shell Finite Element: Two Simple Triangular Shell Element

Cinthia A. G. Sousa[1], Matheus L. Sanchez[1], Gustavo C. Gomes[1], Paulo M. Pimenta[1]

[1]*Polytechnic School at University of São Paulo*
Av. Prof. Almeida Prado, trav.2 nº. 83 Edifício Paula Souza, 05424-970, São Paulo, Brazil
cinthia.sousa@usp.br, matheus.sanchez@usp.br, gustavocanario@gmail.com, ppimenta@usp.br

Abstract. Shells are one of the most important models in solid mechanics since many structures in engineering may be associated with it: metal sheets-based products, slabs, thin-walled pressure vessels, and other objects with one of its dimensions considerably smaller than others. Shell models may be adaptable to finite element usage, but some particularities must be watched it, such as locking behaviours.

This work aims to study and develop a nonlinear formulation for shells models using a special simple triangular shell element, which is a new displacement-based triangular shell element with 6 nodes. Moreover, the shear locking and membrane locking behaviour are not observed at the performance of this new element.

In formulation of shell models, we consider finite strains, large displacements, and rotations. Rotation field is re-parameterized in terms of the Rodrigues rotation vector, resulting in a simpler update of rotational variables. The Kirchhoff-Love kinematical assumption and an initial plane reference configuration for the shell is considered here.

A computational implementation is done with several numerical examples using the new element developed here. Furthermore, a comparison with numerical examples using the well-known element T6-3i (Campello et al. [1]), a six parameter (3 displacements and 3 rotations) element, is done with the aim to also illustrate the robustness of our formulation.

Keywords: Triangular Shell Element, Nonlinear Shell Formulation, Finite Rotations, Large Strains.

1 Introduction

In this work we present a new geometrically exact six-parameter shell formulation considering linear interpolation functions and incremental rotation.

Shell formulation the geometrically exact six-parameter shell formulation of Campello et al. [1] that introduce a special triangular shell finite element for the solution of the resultant static boundary value problem. Its approach define energetically conjugated cross sectional stresses and strains, based on the concept of shell director with a standard Kirchhoff-Love kinematical assumption. Appealing is the fact that both the first Piola–Kirchhoff stress tensor and the deformation gradient appear as primary variables. The resulting expressions are much similar to those obtained for geometrically-exact spatial rods in Pimenta and Yojo [2], rendering a very convenient pattern for the simultaneous coding of rod and shell finite elements.

We assume a plane reference configuration for the shell mid-surface and finite rotations are treated here by the Rodrigues formula in a pure Lagrangian way, considering the Rodrigues parameter and incremental rotation. Still in shell, a new displacement-based triangular shell element is furthermore described. The element has 6 nodes and is flat in the reference configuration, with a nonconforming linear rotation field and a compatible quadratic interpolation scheme for the displacements. Furthermore, a computational implementation is done using AceGen and AceFEM in a benchmark example using the new element T3-3i and the consolidated element T6-3i (see more in Campello et al. [1], Campello [3]) for comparison of locking behaviour.

Finally, about the notation considered in throughout the text, italic Latin or Greek lowercase letters $(a, b, ..., \alpha, \beta)$ denote scalars quantities, bold italic Latin or Greek lowercase letters $(\mathbf{a}, \mathbf{b}, ..., \boldsymbol{\alpha}, \boldsymbol{\beta})$ denote vectors, bold italic Latin or Greek capital letters $(\mathbf{A}, \mathbf{B}, ...)$ denote matrix and second order tensors. Summation convention over repeated indices, with values $\{1, 2, 3\}$ for latin letters and $\{1, 2\}$ for greek letters.

2 Shell Formulation

2.1 Kinematics

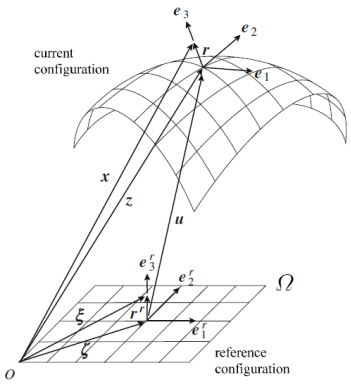

Source: Pimenta et al. [4]

Figure 1. Shell description and basic kinematic quantities.

It is assumed at the initial reference configuration that the middle surface of the shell is plane, as show in Figure (1). In the current configuration an arbitrary point in the shell has its position defined by $\mathbf{x} \in \mathbb{R}^3$, considering the projection in shell middle surface it may be decomposed in $\mathbf{z} \in \Omega \subset \mathbb{R}^3$ and $\mathbf{a} \in \mathbb{R}^3$ representing the perpendicular vector to middle surface. In the reference configuration, this same point position is represented by $\xi \in \mathbb{R}^3$ which is also decomposed in $\zeta \in \Omega^r \subset \mathbb{R}^3$ and $\mathbf{a^r} \in \mathbb{R}^3$. As shown below:

$$\xi = \zeta + \mathbf{a^r} \;\; , \zeta = \xi_\alpha \mathbf{e^r_\alpha}, \quad \xi_\alpha \in \Omega^r \quad and \quad \mathbf{a^r} = \xi_3 \mathbf{e^r_3}, \;\; \xi_3 \in H^r \tag{1}$$

where

$$\mathbf{x} = \mathbf{z} + \mathbf{a}, \;\; \mathbf{z} = \zeta + \mathbf{u}, \;\; \mathbf{a} = s\mathbf{e_3}, \;\; \mathbf{e_3} \;=\; \mathbf{Q}\mathbf{e^r_3} \quad and \quad \mathbf{Q} = \mathbf{e_i} \otimes \mathbf{e^r_i}. \tag{2}$$

Following the same assumptions developed for Sanchez et al. [5], the thickness variation of the shell is implemented using a viable s, such that is possible to define the deformation gradient $\mathbf{F}$ (for more details see Sanchez et al. [5]). Then the curvature vectors and tensor can be defined as

$$\begin{array}{l} \mathbf{K}_\alpha = \mathbf{Q}_{,\alpha}\mathbf{Q^T}, \\ \kappa_\alpha = axial\left(\mathbf{K}_\alpha\right) \end{array} \quad and \quad \begin{array}{l} \kappa_\alpha = \mathbf{\Gamma}_\beta \mathbf{u}_{,\beta\alpha}, \\ \mathbf{\Gamma}_1 = \left(\mathbf{e}_1 \cdot \mathbf{z}_{,1}\right)^{-1}[Skew\left(\mathbf{e}_1\right) - \left(\mathbf{e}_1 \cdot \mathbf{z}_{,2}\right)\left(\mathbf{e}_2 \cdot \mathbf{z}_{,2}\right)^{-1}(\mathbf{e}_1 \otimes \mathbf{e}_3)] \\ \mathbf{\Gamma}_2 = \left(\mathbf{e}_2 \cdot \mathbf{z}_{,2}\right)^{-1}\left(\mathbf{e}_1 \otimes \mathbf{e}_3\right) \end{array} \tag{3}$$

Previously, we have

$$\mathbf{f}_\alpha = \mathbf{z}_{,\alpha} + s_{,\alpha}\mathbf{Q}\mathbf{e^r_3} \;+\; s\mathbf{Q}_{,\alpha}\mathbf{e^r_3} = \mathbf{z}_{,\alpha} + s_{,\alpha}\mathbf{e_3} + \kappa_\alpha \times \mathbf{a} \quad and \quad \mathbf{f_3} = s_{,3}\mathbf{Q}\mathbf{e^r_3} \tag{4}$$

Let now the Back-rotated counterparts of $\mathbf{F}$ and strains be

$$\mathbf{F}^r = \mathbf{Q^T}\mathbf{F} = \mathbf{I} + \gamma^r_\alpha \otimes \mathbf{e}^r_\alpha + \gamma^r_{33} \otimes \mathbf{e}^r_3 \quad and \quad \begin{cases} \mathbf{e}^r_\alpha + \gamma^r_\alpha = \mathbf{Q^T}(\mathbf{z}_{,\alpha} + s_{,\alpha}\mathbf{e_3} + \kappa_\alpha \times \mathbf{a}) \\ \mathbf{e}^r_3 + \gamma^r_{33} = \mathbf{Q^T}(s_{,3}\mathbf{e_3}) \end{cases} \tag{5}$$

Afterwards the strains at current and reference configurations can be given by

$$\begin{cases} \gamma^r_\alpha = \eta^r_\alpha + \mathbf{k}^r_\alpha \times \mathbf{a}^r \\ \gamma^r_{33} = (s_{,3} - 1)\mathbf{e}^r_3 \end{cases}, \quad where \quad \begin{array}{l} \eta^r_\alpha = \mathbf{Q}^T\mathbf{z}_{,\alpha} + s_{,\alpha}\mathbf{e}^r_3 - \mathbf{e}^r_\alpha \\ \kappa^r_\alpha = \text{axial}\left(\mathbf{Q}^T\mathbf{Q}_{,\alpha}\right) \end{array} \tag{6}$$

and

$$\begin{cases} \gamma_\alpha = \eta_\alpha + \mathbf{k}_\alpha \times \mathbf{a} \\ \gamma_{33} = (s_{,3} - 1)\,\mathbf{e_3} \end{cases}, \quad where \quad \begin{array}{l} \eta_\alpha = \mathbf{z}_{,\alpha} + s_{,\alpha}\mathbf{e_3} - \mathbf{e}_\alpha \\ \kappa_\alpha = axial(\mathbf{Q}_{,\alpha}\mathbf{Q^T}) \end{array}. \tag{7}$$

2.2 Weak form of equilibrium and constitutive equations

In this work the virtual work theorem is considered to develop the shell finite element model, as follows

$$\delta \mathrm{W} = \delta W_{\mathrm{int}} - \delta W_{\mathrm{ext}} = 0 \ , \ \forall \delta \mathbf{u} \quad and \quad \begin{array}{l} \delta \mathrm{W}_{\mathrm{int}} = \int_B \mathbf{P} : \delta \mathbf{F} \mathrm{dV} = \int_{\Omega^r} (\sigma^{\mathbf{r}}_\alpha \cdot \delta \varepsilon^{\mathbf{r}}_\alpha) \mathrm{d}\Omega^{\mathrm{r}} \\ \delta \mathrm{W}_{\mathrm{ext}} = \int_{\partial B} \overline{\mathbf{t}} \cdot \delta \mathbf{x} \mathrm{dA} + \int_B \overline{\mathbf{f}} \cdot \delta \mathbf{x} \mathrm{dV} \end{array} . \tag{8}$$

with

$$\sigma^{\mathbf{r}}_\alpha = \left[\begin{array}{cc} \mathbf{n}^r_\alpha & \mathbf{m}^r_\alpha \end{array} \right]^T \quad and \quad \varepsilon^{\mathbf{r}}_\alpha = \left[\begin{array}{cc} \eta^r_\alpha & \kappa^r_\alpha \end{array} \right]^T . \tag{9}$$

The following strain energy function is considered for elastic material

$$\psi = \frac{1}{2}\lambda \left(\frac{1}{2} \left(J^2 - 1 \right) - \ln \left(J \right) \right) + \frac{1}{2}\mu \left(I_1 - 3 - 2 \ln \left(J \right) \right) \ . \tag{10}$$

where λ and μ are Lamé coefficients and I_i are the invariants of the Cauchy-Green tensor defined by

$$I_1 = \mathrm{tr}\ \mathbf{C} = \mathbf{f}_i \cdot \mathbf{f}_i, \quad I_2 = \mathrm{tr}\left[\mathrm{Cof}\ \mathbf{C} \right] = \mathbf{g}_i \cdot \mathbf{g}_i \quad and \quad I_3 = \det \mathbf{C} = J^2 = \left(\mathbf{f}_1 \cdot \left(\mathbf{f}_2 \times \mathbf{f}_3 \right) \right)^2 . \tag{11}$$

2.3 Rotation Field

The Rodrigues parametrization is done following the works of Pimenta et al. [6] and Silva [7]. The Rodrigues rotation parameters may be defined by

$$\boldsymbol{\alpha} = \alpha \mathbf{e} \tag{12}$$

where, $\boldsymbol{\theta}$ is the Rodrigues rotation vector and the scalar α is given by

$$\alpha = \tan \frac{\theta}{2} \quad with \quad 0 \leq \theta < \pi \tag{13}$$

The rotation tensor $\mathbf{Q}$ in terms of the tensor $\mathbf{A}$ is given by the so-called Cailey transform, considering geometric using vector properties, renders

$$\mathbf{Q} = \left(\mathbf{I} - \frac{\mathbf{A}}{\mathbf{2}} \right)^{-\mathbf{1}} \left(\mathbf{I} + \frac{\mathbf{A}}{\mathbf{2}} \right) \tag{14}$$

After some mathematical manipulation (for more details, see Silva [7]), and considering another rotation parameter $\boldsymbol{\alpha} = \widehat{\boldsymbol{\alpha}} \left(\mathbf{u}', \varphi \right)$, can be considered the following expression for rotation parameter

$$\boldsymbol{\alpha} = \|\mathbf{e}^{\mathbf{m}}_{\mathbf{3}}\|^{-2} (\mathbf{e}^{\mathbf{r}}_{\mathbf{3}} \times \mathbf{e}_{\mathbf{3}}) + \varphi \|\mathbf{e}^{\mathbf{m}}_{\mathbf{3}}\|^{-\mathbf{1}} \mathbf{e}^{\mathbf{m}}_{\mathbf{3}}. \tag{15}$$

It's necessary to consider the rotation incrementally because with the Rodrigues parameters we would have a singularity at π and $-\pi$, so if it was done it by increments, then the increment will be sufficiently small so we can bypass this problem. Therefore, its possible to get the updated alpha just with the last step

$$\boldsymbol{\alpha}_\Delta = \|\mathbf{e}^{\mathbf{m}}_{\mathbf{3}}\|^{-2} \left(\mathbf{e}^{\mathbf{i}}_{\mathbf{3}} \times \mathbf{e}^{\mathbf{i+1}}_{\mathbf{3}} \right) + \varphi_\Delta \|\mathbf{e}^{\mathbf{m}}_{\mathbf{3}}\|^{-1} \mathbf{e}^{\mathbf{m}}_{\mathbf{3}} \tag{16}$$

and the incremental alpha vectors which is also appealing, because it makes it easy to update

$$\boldsymbol{\alpha}_{i+1} = \frac{4}{4 - \boldsymbol{\alpha}_i \cdot \boldsymbol{\alpha}_\Delta} \left(\boldsymbol{\alpha}_i + \boldsymbol{\alpha}_\Delta - \frac{1}{2} \boldsymbol{\alpha}_i \times \boldsymbol{\alpha}_\Delta \right). \tag{17}$$

A C^1 continuity between the finite elements must be assured because of the Kirchhoff–Love's assumption that the deformation gradient of the shell is written in terms of first- and second-order derivatives of the displacements. In this work, this condition is imposed considering the rotation parameter $\boldsymbol{\alpha}_\Delta$ a penalty approach and by a Lagrange multiplier, which enforces the equality at the kinking of the edge of two neighboring elements (for more details, see Sanchez et al. [5]).

$$\boldsymbol{\alpha}_\Delta = \frac{-2}{1 + \mathbf{e}^{\mathbf{i+1}}_{\mathbf{k}} \cdot \mathbf{e}^{\mathbf{i}}_{\mathbf{k}}} \mathbf{e}^{\mathbf{i+1}}_{\mathbf{j}} \times \mathbf{e}^{\mathbf{i}}_{\mathbf{j}} \quad \textbf{and} \quad \varphi_{\boldsymbol{\Delta}} = \boldsymbol{\alpha}_{\boldsymbol{\Delta}} \cdot \frac{\mathbf{e}^{\mathbf{m}}_\tau}{\|\mathbf{e}^{\mathbf{m}}_\tau\|}. \tag{18}$$

3 Finite Element Implementation

The shell elements in this work is inspired at the T6-3i element [1] that is a 6-node displacement-based one. In this model, the T6-3i a standard compatible quadratic displacement field is placed on all nodes, while a linear interpolation scheme for the rotation vector $\boldsymbol{\alpha}$ is set only on the mid-sides. The absence of rotational degrees-of-freedom in the corner nodes makes the T6-3i a nonconforming element with respect to the rotation field.

The first element we consider, that is object of my PhD research, is the new simplest triangular shell element of six nodes named T3-3i. This element is plane in the reference configuration. In this element there are placed 3 nodes of displacements DOF's and 3 nodes of rotation DOF's as can be seen in Fig. 2 below.

In this work, it was considerations that is considered 3 integration points at mid-side nodes, linear displacement Field ($\mathbf{u}$), linear incremental Non-Conform Rotation Field (α_Δ), enforcement of Rotation continuity and Rotation Field with no Drilling degrees-of-freedom.

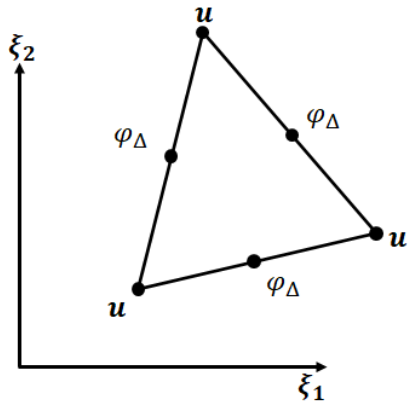

Figure 2. The T3-3iKL element.

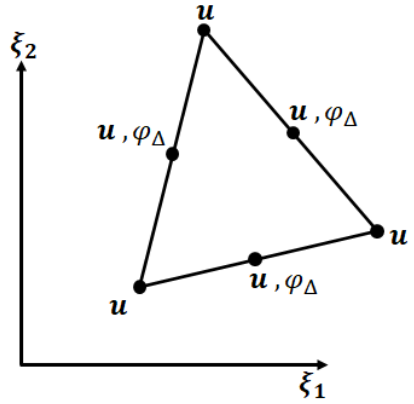

Figure 3. The T6-3iKL element.

The other element considered here is the T6-3iKL element (see Fig. 3) developed in Sanchez et al. [5]. In this element is assumed that are 3 integration points at mid-side nodes and Quadratic Displacement Field. The linear incremental Non-Conform Rotation Field α_Δ is built with considerations to φ_Δ and $\mathbf{u}$, the enforcement of Rotation continuity is considered and the Rotation Field with no Drilling degrees-of-freedom.

4 Results

The finite element model developed here has been implemented in AceGen / AceFEM platform (see Korelc [8]). Two simple and popular cases were tested the Cantiliever Beam and Pinchided Cylinder.

4.1 Cantilever Beam

The cantilever problem here is three dimensional which leads to a classical buckling problem and squared cross-section is subjected to a large point load at the center of its free end. The simulation has been executed for different mesh discretization and for different thicknesses in order to analyze the FEM model built in this article. The results are compared to shell FEM model from Campello et al. [1].

The geometrical parameters adopted can be seen in Fig. 4 and material parameter considered was the anisotropic material. The beam is subject to vertical down force up to $F_y = 10000N$ and an horizontal perturbation force is also introduced ($F_z = F_y \cdot 10^{-4}$) in order to induce the buckling phenomena.

Two different situations are enforced here: (i) in-plane bending with the load applied in the same plane of the beam and (ii) out-of plane bending with the load applied in the out-of-plane direction.

With this simple example we want to show that the developed approach is capable to undergo large in-plane and out-of plane rotations using both elements T6-3i, see Fig. 5, and T3-3i in Fig. 6, respectively.

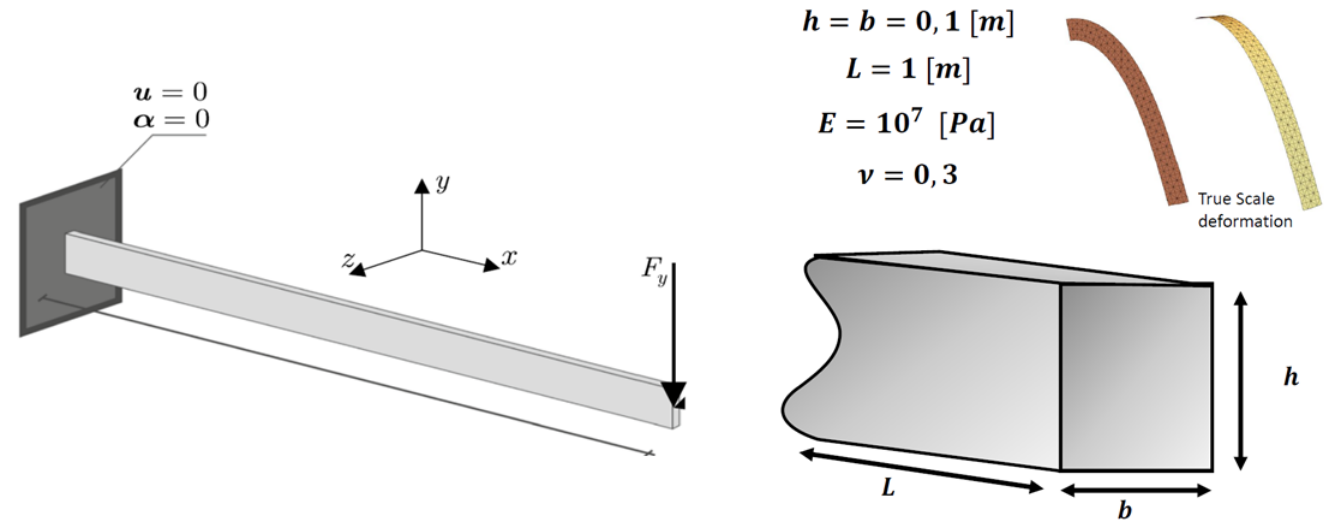

Figure 4. Cantilever Beam

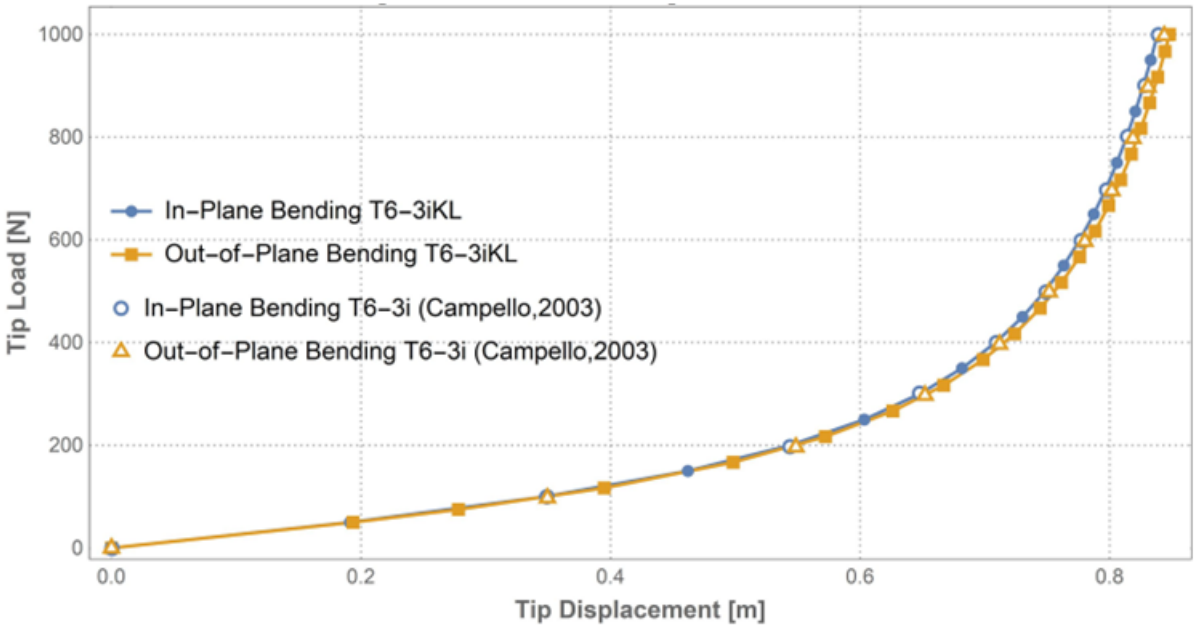

Figure 5. T6-3iKL: Tip load versus Tip deflection

4.2 Pinched Cylinder

This example is a good benchmark to evaluate the shell model for big displacements and curvatures. It consists of a cylinder with rigid ends and subject to a radial vertical force in its center. This simulation scenario has been based on the articles Campello et al. [1], Pimenta and Campello [9] and Silva [7]. Here, a thin cylinder is subject to a radial vertical force in its center, the scheme of boundary value problem and the geometrical parameters adopted can be seen in Fig. 7.

The Figures above illustrates the vertical displacement of point A and the horizontal displacement of point B for different load factors. Each line in the graphics represents a different Finite element model. Results from some

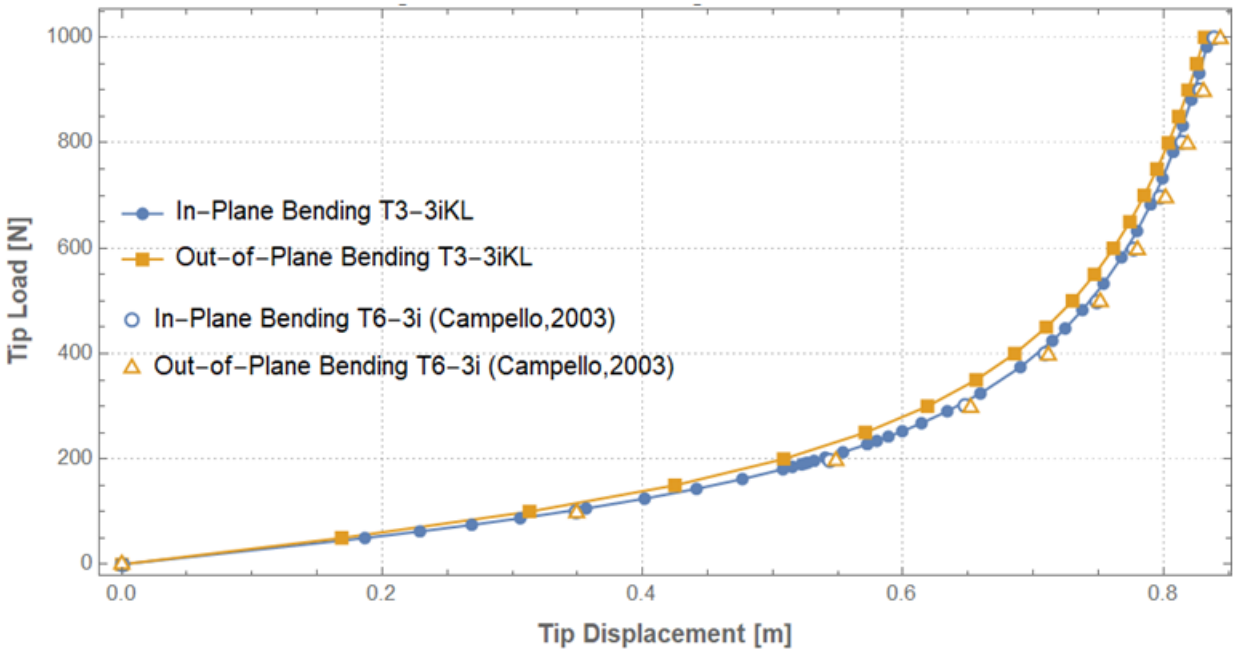

Figure 6. T3-3iKL: Tip load versus Tip deflection

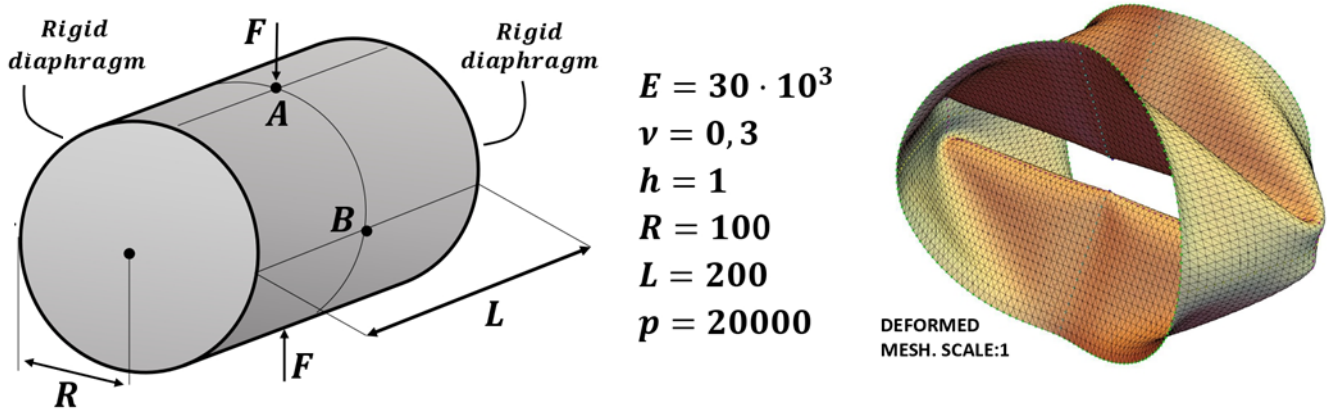

Figure 7. Pinched Cylinder

sources in bibliography have been plotted in the same Graph for comparison.

5 Conclusions

The research results obtained so far demonstrates the reliability of the element developed. The authors believe that the simplicity of the kinematic in this geometrically exact nonlinear model, together with its capacity to simulate thin structures in large displacements, large rotations and for possibly different material models, makes this element appealing for further development. In further research yet to come, the authors are going to enhance the element T3-3i to several examples and for dynamic simulations and for non-isotropic materials (for example composites).

Acknowledgements. Cinthia A. G Sousa acknowledges the fund support by CNPq (contract/grant number: 140108/2022-0) and all the authors thankfully acknowleges the Fapesp (contract/grant number: 2020/13362-1).

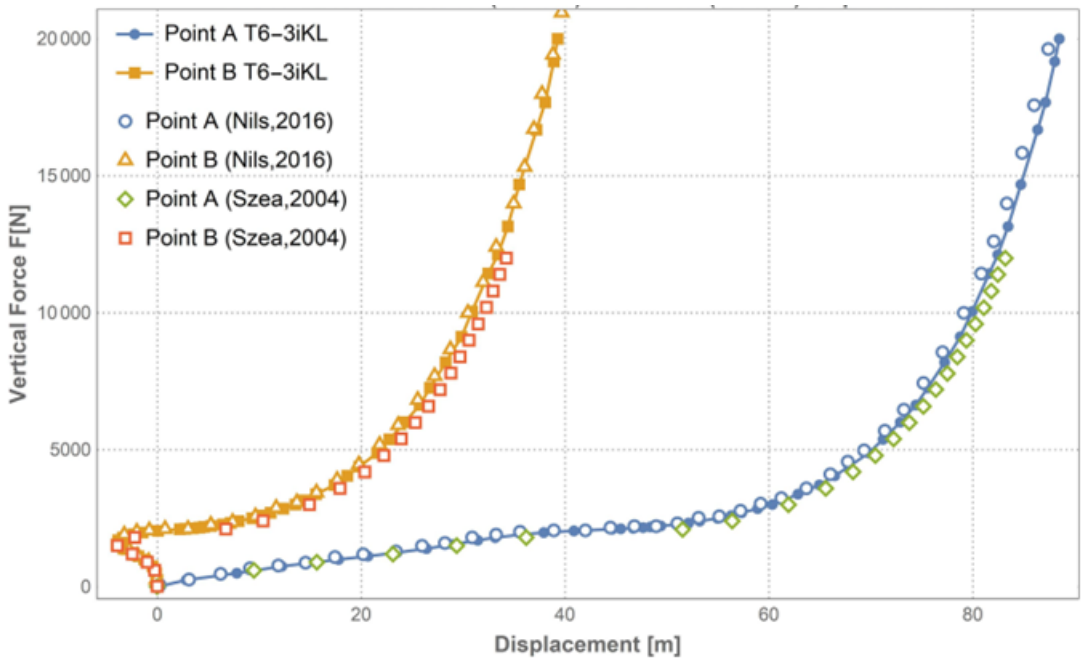

Figure 8. Vertical force versus vertical (point A) and lateral (point B) displacement

Authorship statement. The authors hereby confirm that they are the sole liable persons responsible for the authorship of this work, and that all material that has been herein included as part of the present paper is either the property (and authorship) of the authors, or has the permission of the owners to be included here.

References

[1] E. M. Campello, P. M. Pimenta, and P. Wriggers. A triangular finite shell element based on a fully nonlinear shell formulation. *Computational Mechanics*, vol. 31, pp. 505–518, 2003.

[2] P. M. Pimenta and T. Yojo. Geometrically exact analysis of spatial frames. *Applied Mechanics Reviews*, vol. 46, pp. S118–S128, 1993.

[3] E. M. B. Campello. *Modelos não-lineares de casca em elasticidade e elastoplasticidade com grandes deformações: teoria e implementação em elementos finitos*. Phd theses, Escola Politécnica da Universidade de São Paulo, São Paulo. , 2005.

[4] P. M. Pimenta, E. M. Campello, and P. Wriggers. A fully nonlinear multi-parameter shell model with thickness variation and a triangular shell finite element. *Computational Mechanics*, vol. 34, pp. 181–193, 2004.

[5] M. L. Sanchez, e C. C. Silva, and P. M. Pimenta. A simple fully nonlinear kirchhoff-love shell finite element. *Latin American Journal of Solids and Structures [online]*, vol. 17, 2020.

[6] P. M. Pimenta, E. M. Campello, and P. Wriggers. An exact conserving algorithm for nonlinear dynamics with rotational dofs and general hyperelasticity. part 1: Rods. *Computational Mechanics*, vol. 42, pp. 715–732, 2008.

[7] C. C. Silva. *Geometrically exact shear-rigid shell and rod models.* PhD thesis, Universidade de São Paulo, 2020.

[8] W. P. J.A.. Korelc. *Automation of Finite Element Methods.* Springer, 2016.

[9] P. M. Pimenta and E. M. Campello. Shell curvature as an initial deformation: A geometrically exact finite element approach. *International Journal for Numerical Methods in Engineering*, vol. 78, pp. 1094–1112, 2009.